

Analysis and Control of CAR-T Cell Models

Lakshmi N Sridhar*

Chemical Engineering Department, University of Puerto Rico, Mayaguez, PR 00681, USA

Citation: Sridhar LN. Analysis and Control of CAR-T Cell Models. *J Petro Chem Eng* 2025;3(1):110-119.

Received: 11 March, 2025; Accepted: 17 March, 2025; Published: 19 March, 2025

*Corresponding author: Lakshmi N Sridhar, Chemical Engineering Department, University of Puerto Rico, Mayaguez, PR 00681, USA, E-mail: lakshmin.sridhar@upr.edu

Copyright: © 2025 Sridhar LN., This is an open-access article published in *J Petro Chem Eng* (JPCE) and distributed under the terms of the Creative Commons Attribution License, which permits unrestricted use, distribution, and reproduction in any medium, provided the original author and source are credited.

ABSTRACT

CAR T-cell therapy is a new type of cancer treatment that uses the immune system to kill cancer cells. In many situations, it has cured people where all other treatments have failed. The interaction between the CAR T cells and the cancer cells is very complex and highly nonlinear and to get the best results, one must consider several factors. This work involves the development of a rigorous mathematical framework to deal with the high degree of complexity that exists in the interaction between CAR-T cells and cancer. Bifurcation analysis and Mult objective nonlinear model predictive control (MNLMP) calculations were performed on CAR-T cell models describing the interaction between CAR-T and the cancerous cells. The MATLAB program MATCONT was used to perform the bifurcation analysis. The MNLMP calculations were performed using the optimization language PYOMO in conjunction with the state-of-the-art global optimization solvers IPOPT and BARON. The bifurcation analysis revealed limit points branch points and Hopf bifurcation points. The Hopf bifurcation points that cause unwanted limit cycles were eliminated using an activation factor involving the tanh function. The limit and branch points were beneficial because they allowed the Mult objective nonlinear model predictive control calculations to converge to the Utopia point which is the most beneficial solution.

Keywords: Bifurcation; optimization; control; cancer tumor; CAR-T cells

Background

Boer, et al¹, investigated recruitment times, proliferation and apoptosis rates during the cd8+ t-cell response to the lymphocytic choriomeningitis virus. Rustom Antia, et al^{2,3}, developed models of cd8+ responses and analyzed the role of models in understanding cd8+ t-cell memory. Lisette G de Pillis, et al⁴, developed a validated mathematical model of cell-mediated immune response to tumor growth. Brentjens, et al⁵, researched the treatment of chronic lymphocytic leukemia with genetically targeted autologous T cells. Kalos M, et al⁶, showed that C.H. T cells with chimeric antigen receptors have potent antitumor effects and can establish memory in patients with advanced leukemia. Kochenderfer, et al⁷, demonstrated B-cell depletion and malignancy remissions along with cytokine-

associated toxicity in a clinical trial of anti-CD19 chimeric-antigen-receptor transduced T cells. Grupp, et al⁸, researched Chimeric antigen receptor-modified T cells for acute lymphoid leukemia. De Boer and Perelson⁹, quantified t lymphocyte turnover. Dotti, et al¹⁰, designed and developed therapies using chimeric antigen receptor-expressing T cells. Davenport, et al¹¹, argued that CAR-T cells are serial killers. Brown, et al^{12,13}, demonstrated the regression of glioblastoma after chimeric antigen receptor t-cell therapy optimized il13ra2-targeted chimeric antigen receptor t-cells for improved persistence and antitumor efficacy against glioblastoma. Hege, et al¹⁴, investigated the safety, tumor trafficking and immunogenicity of chimeric antigen receptor (car)-t cells specific for tag-72 in colorectal cancer. Davenport, et al¹⁵, extracted chimeric antigen

receptor T cells form nonclassical and potent immune synapses driving rapid cytotoxicity. Mostolizadeh, et al¹⁶, developed a mathematical model of chimeric antigen receptor (CAR) T cell therapy with presence of cytokine. Andrew M Stein, et al¹⁷, investigated tisagenlecleucel model-based cellular kinetic analysis of chimeric antigen receptor-t cells. Nirali N Shah and Terry J Fry¹⁸, developed mechanisms of resistance to CAR T cell therapy. Feins, et al¹⁹, provided an introduction to chimeric antigen receptor (car) t-cell immunotherapy for human cancer. Ghorashian, et al²⁰, researched enhanced car t cell expansion and prolonged persistence in pediatric patients all treated with a low-affinity. Chavez, et al²¹, discussed car t-cell therapy for b-cell lymphomas. Bodnar, et al²², produced a mathematical analysis of a generalized model of chemotherapy for low grade gliomas. Barros, et al²³, discussed some CAR-T cell mathematical models. Anwasha Chaudhury, et al²⁴, reviewed cellular kinetic-pharmacodynamic modeling approaches. Laetitia Vercellino, et al²⁵, discussed the various predictive factors of early progression after car t-cell therapy in large b-cell lymphoma. Altrock, et al²⁶, discussed the roles of t cell competition and stochastic extinction events in chimeric antigen receptor t cell therapy. Can Liu, et al²⁷, provided a Model-based cellular kinetic analysis of chimeric antigen receptor-t cells in humans. Alvaro Martinez-Rubio, et al²⁸, provided a mathematical description of the bone marrow dynamics during car t-cell therapy in b-cell childhood acute lymphoblastic leukemia. Barros, et al²⁹, developed a mathematical model of CAR-T immunotherapy in preclinical studies of hematological cancers. Anna Mueller-Schoell, et al³⁰, developed an early survival prediction framework in cd19-specific car-t cell immunotherapy using a quantitative systems pharmacology model. Aman P Singh, et al³¹, produced a bench-to-bedside translation of chimeric antigen receptor (car) t cells using a multiscale systems pharmacokinetic-pharmacodynamic model. Victor M Perez-Garcia, et al³², produced insights from mathematical models of car t cells for t-cell leukemias. Kimmel, et al³³, investigated the roles of T cell competition and stochastic extinction events in chimeric antigen receptor T cell therapy. León-Triana et al³⁴, showed that dual-target car-ts with on- and off-tumor activity may override immune suppression in solid cancers: a mathematical proof of concept. Cancers 13(4), 703. León-Triana³⁵, provided insights from mathematical models of Car t cell therapy in b-cell acute lymphoblastic leukaemia. Liu, et al³⁶, developed a model-based cellular kinetic analysis of chimeric antigen receptor-T cells in humans. Martinez-Rubio, et al³⁷, provided a mathematical description of the bone marrow dynamics during car t-cell therapy in b-cell childhood acute lymphoblastic leukemia. Nukala, et al³⁸, provided a systematic review of the efforts and hindrances of modeling and simulation of CAR T-cell therapy while Owens, et al³⁹, modeled CAR T-cell therapy with patient preconditioning. Valle, et al⁴⁰, discussed eradication conditions and in silico experimentation for CAR-T cell therapy Santurio and Barros, et al⁴¹, developed a mathematical model for on-target off-tumor effect of car-t cells on gliomas. Emanuelle, et al⁴², modeled patient-specific car-t cell dynamics and discussed multiphasic kinetics via phenotypic differentiation. Ahmed M Salem, et al⁴³, developed a multiscale mechanistic modeling framework integrating differential cellular kinetics of car t-cell subsets and immunophenotypes in cancer patients. Daniel C Kirouac, et al⁴⁴, discussed the deconvolution of clinical variance in car-t cell pharmacology and response. Bodnar, et al⁴⁵, analyzed a mathematical model of car-t cell therapy for glioblastoma Daniela Silva Santurio,

et al⁴⁶, discussed the various mechanisms of resistance to car-t cell immunotherapy and provided insights from a mathematical model. Sergio Serrano, et al⁴⁷, discussed the role of b-cells in car t-cell therapy in leukemia through a mathematical model. Daniela S Santurio⁴⁸, showed that the mathematical modeling unveils the timeline of car-t cell therapy and macrophage-mediated cytokine release syndrome.

Motivation and Objectives

Although several CAR-T Cell models have been developed, bifurcation analysis and optimal control calculations have been disjointly done. Additionally, all optimal control calculations involve single objective minimization. The main objective of this work is to perform bifurcation analysis in conjunction with multiobjective nonlinear model predictive control on CAR-T Cell models demonstrating the effects of bifurcation analysis on multiobjective nonlinear model predictive control. This paper is organized as follows. First, the description of the problems involving CAR T cells is presented. The results and discussion then follow a discussion of the numerical techniques that involve bifurcation analysis and multiobjective nonlinear model predictive control.

Description of Problems Involving Car-T Cells

The first problem is described in Fassoni, et al⁴⁹, while the second and third are presented in Khailov, et al⁵⁰ and Bodnar, et al⁵¹.

Problem 1

In problem 1⁴⁹ the dynamic model involving the CAR-T Cells is

$$\begin{aligned} \frac{dC_T}{dt} &= r_{\min} \frac{T}{A+T} C_T - (\xi + \varepsilon + \Lambda) C_T + \theta T C_M - \alpha T C_T \\ \frac{dC_M}{dt} &= \varepsilon C_T - \theta T C_M - \mu C_M \\ \frac{dT}{dt} &= rT(1-bT) - \gamma T \frac{C_T}{a + \delta T + C_T} \end{aligned} \quad (1)$$

C_T, C_M, T are the effector CAR-T cells, memory CAR-T cells and tumor cells. r is the basal expansion rate of the effector CAR-T cells. θ represents the rate at which the effector cells transition to the memory cells while ε is the rate at which the effector cells are exhausted. μ represent the death rates of effector, memory and exhausted CAR-T cells. The logistic growth rate of tumor cells is r and the carrying capacity is $1/b$. The rate of cytotoxic effects on the tumor cells is γ . The mass-action law models the immunosuppressive effect on the effector CAR-T cells with a constant. This set of equations was scaled and results in

$$\begin{aligned} \frac{dax}{d\tau} &= pa \frac{ax(az)}{k+z} - w(ax) + q(az)ay - u(ax)ax \\ \frac{day}{d\tau} &= s(ax) - q(az)ay - mq(ay) \\ \frac{daz}{d\tau} &= az(1-az) - v \frac{ax(az)}{c+ax+az} \end{aligned} \quad (2)$$

$$ax = \frac{b}{d}C_T, ay = \frac{b}{d}C_M, az = bT, k = bA, q = \frac{\theta}{rb}, s = \frac{\varepsilon}{r}, c = \frac{ab}{d}$$

$$\tau = rt, pa = \frac{r_{\min}}{r}, u = \frac{\alpha}{rb}, w = \frac{(\xi + \varepsilon + \Lambda)}{r}, m = \frac{\mu b}{\theta} \quad (3)$$

The parameter values are $v = 289/20$; $w = 1/2$; $m = 3/20$; $k = 3/20$; $c = 3/20$; $q = 9/20$; $s = 9/20$; $u = 0.2$. pa is the bifurcation parameter and the control value.

Problem 2

In this problem Khailov, et al⁵⁰ the dynamic equations are

$$\frac{dxa}{dt} = rxa(t) - \alpha_1 xa(t) ya(t) - \beta_1 xa(t) za(t) + \mu xa(t)$$

$$\frac{dya}{dt} = (pval) ya(t) - \eta (ya(t))^2 - \alpha_2 xa(t) ya(t) - \beta_2 ya(t) za(t)$$

$$\frac{dza}{dt} = qza(t) - \gamma (za(t))^2 - \alpha_3 xa(t) za(t) - \beta_3 ya(t) za(t)$$

$$\frac{dwa}{dt} = \lambda - v wa(t) + nval(1 - vval) wa(t) xa(t) \quad (3)$$

$$r = 0.6; pval = 1.1; \eta = 0.9; \gamma = 1.1; nval = 1; vval = 0.3$$

$$\alpha_1 = 1.0; \alpha_2 = 0.8; \alpha_3 = 0.9; \beta_1 = 0.9; \beta_2 = 0.9; \beta_3 = 1.1;$$

xa, ya, za, wa represent the population of CAR-modified T-lymphocytes, the population of B-leukemic or cancer cells, the population of healthy B-cells and inflammatory cytokines which are elevated by immunotherapy.

$r, pval, q$ represent the growth rate of xa, ya, za $\alpha_1, \alpha_2, \alpha_3$ the relative compatibility coefficients while $\beta_1, \beta_2, \beta_3$ are the competition coefficients. $\frac{\eta}{pval}, \frac{\gamma}{q}$ represent the per capita growth rates and reciprocal carrying capacities of ya, za . v is the cytokine decay rate. bounded control $vval$ is the control term that plays the role of the intensity of the dosage of immunosuppressant drug intake. $nval$ is a tuning factor that can increase or decrease $(1 - vval) wa(t) xa(t)$. q is the bifurcation parameter and the control variable.

Problem 3

For the third problem Bodnar, et al⁵¹, $\tilde{T}, \tilde{C}, \tilde{P}, \tilde{B}$ represent the tumor cells, the CAR-T Cells in the tumor site, the CAR-T Cells outside the tumor site and the B-Cells which represent the second antigen in the dual-target treatment. The dynamic model equations are

$$\frac{d\tilde{T}}{d\tilde{t}} = (\tilde{\rho}_T (1 - \frac{\tilde{T}}{\tilde{K}}) - \tilde{\alpha}_T \tilde{C}) \tilde{T}$$

$$\frac{d\tilde{C}}{d\tilde{t}} = \tilde{k} \tilde{P} + \tilde{\rho}_C \frac{\tilde{C} \tilde{T}}{g_T + \tilde{T}} - \tilde{\alpha}_C \frac{\tilde{C} \tilde{T}}{g_C + \tilde{C}} - \frac{\tilde{C}}{\tau_C}$$

$$\frac{d\tilde{P}}{d\tilde{t}} = \tilde{A} + \frac{\tilde{\rho}_P \tilde{P} \tilde{B}}{g_B + \tilde{B}} - \frac{\tilde{P}}{\tau_P} - \tilde{k} \tilde{P}$$

$$\frac{d\tilde{B}}{d\tilde{t}} = -\tilde{\alpha}_B \tilde{P} \tilde{B} - \frac{\tilde{B}}{\tau_B} \quad (4)$$

$\tilde{\rho}_C$ (Mitotic stimulation of CAR-T cells by tumor cells) = 0.9; g_C (CAR-T concentration for half-maximal tumor inactivation) = 2.e+09; $\tilde{\alpha}_C$ (Tumor inactivation rate) = 0.05; τ_C (Activated CAR-T cell mean lifetime in the tumor site) = 7; $\tilde{\rho}_T$ (Tumour growth rate) = 0.01; g_T (Tumour cells concentration for half-maximal CAR-T cell proliferation) = 1.e+10; $\tilde{\alpha}_T$ (CAR-T cells killing efficiency against tumor) = 2.5e-10; $\tilde{\rho}_P$ (Mitotic stimulation of CAR-T cells by the antigen cells) = 0.9; τ_P (Activated CAR-T cell mean lifetime outside the tumor site) = 7; g_B (B-cell concentration for half-maximal CAR-T cell proliferation) = 1.e+10; $\tilde{\alpha}_B$ (9CAR-T cells induced B cell death rate) = 1.e-11; τ_B (B cell mean lifetime) = 45; \tilde{k} (CAR-T cells infiltrating the tumor site rate) = 0.2; \tilde{K} (Tumour carrying capacity) = 2.e+12; \tilde{A} (CAR-T cell dosage) = 2.8571e+06;

This set of equations is scaled using the following transformations.

$$t = \frac{\tilde{t}}{\tau_C}; pval = \frac{\tilde{P}}{g_C}; tval = \frac{\tilde{T}}{g_T}; cval = \frac{\tilde{C}}{g_C}; bval = \frac{\tilde{B}}{g_B};$$

$$\rho_T = \tilde{\rho}_T \tau_C; \rho_P = \tilde{\rho}_P \tau_C; \alpha_T = \tilde{\alpha}_T g_C \tau_C; \eta_b = \frac{\tau_C}{\tau_B}; k = \tilde{k} \tau_C; a = \tilde{A} \tau_C;$$

$$b = \frac{\tilde{\alpha}_C g_T \tau_C}{g_C}; \alpha_b = \tilde{\alpha}_B g_C \tau_C; \eta_p = \tau_C (\frac{1}{\tau_P} + \tilde{k}); aval = \tilde{A} \frac{\tau_C}{g_C}$$

Using these transformations the dynamic model would become

$$\frac{dtval}{dt} = \rho_T (1 - \frac{tval}{k}) - \alpha_T (cval) (tval)$$

$$\frac{dcval}{dt} = k (pval) + aval (tval / (1 + tval)) - b * (tval / (1 + cval) - 1) cval$$

$$\frac{dpval}{dt} = (aval + \rho_P bval / (1 + bval) - \eta_p) pval$$

$$\frac{dbval}{dt} = -(\alpha_b pval + \eta_b) bval \quad (5)$$

Numerical Methods

Bifurcation analysis

The existence of multiple steady-states and limit cycles in various processes has led to much research involving bifurcation analysis. Multiple steady states occur because of the existence of branch and limit points. Hopf bifurcation points cause limit cycles.

One of the most commonly used software to locate limit points, branch points and Hopf bifurcation points is the MATLAB program MATCONT (Dhooge Govearts and Kuznetsov⁵²; Dhooge Govearts, Kuznetsov, Mestrom and Riet⁵³). This software detects Limit points (LP), branch points (BP) and Hopf bifurcation points (H). Consider an ODE system

$$\frac{dx}{dt} = f(x, \alpha) \quad (6)$$

$x \in R^n$ Let the tangent plane at any point x be $W = [W_1, W_2, W_3, W_4, \dots, W_{n+1}]$. Define matrix A given by

$$A = \begin{bmatrix} \frac{\partial f_1}{\partial x_1} & \frac{\partial f_1}{\partial x_2} & \frac{\partial f_1}{\partial x_3} & \frac{\partial f_1}{\partial x_4} & \dots & \frac{\partial f_1}{\partial x_n} & \frac{\partial f_1}{\partial \alpha} \\ \frac{\partial f_2}{\partial x_1} & \frac{\partial f_2}{\partial x_2} & \frac{\partial f_2}{\partial x_3} & \frac{\partial f_2}{\partial x_4} & \dots & \frac{\partial f_2}{\partial x_n} & \frac{\partial f_2}{\partial \alpha} \\ \dots & \dots & \dots & \dots & \dots & \dots & \dots \\ \frac{\partial f_n}{\partial x_1} & \frac{\partial f_n}{\partial x_2} & \frac{\partial f_n}{\partial x_3} & \frac{\partial f_n}{\partial x_4} & \dots & \frac{\partial f_n}{\partial x_n} & \frac{\partial f_n}{\partial \alpha} \end{bmatrix} \quad (7)$$

The bifurcation parameter is the matrix A can be expressed as

$$A = [\partial f / \partial x \quad | \quad \partial f / \partial \alpha] \quad (8)$$

Where $\partial f / \partial x$ is the Jacobian matrix. Since the gradient is orthogonal to the tangent vector,

$$Aw = 0 \quad (9)$$

For both limit and branch points the matrix $[\partial f / \partial x]$ must be singular. For a limit point (LP) the $n+1^{\text{th}}$ component of the tangent vector $W_{n+1} = 0$ and for a branch point (BP) the matrix

$$\begin{bmatrix} A \\ w^T \end{bmatrix} \text{ must be singular. At a Hopf bifurcation point,} \\ \det(2f_x(x, \alpha) @ I_n) = 0 \quad (10)$$

@ indicates the bi alternate product while is the n-square identity matrix. Hopf bifurcations cause limit cycles and should be eliminated because limit cycles make optimization and control tasks very difficult. More details can be found in Kuznetsov^{54,55} and Govaerts⁵⁶.

Nonlinear model predictive control

The Mult objective nonlinear model predictive control (MNL MPC) method⁵⁷ used in these calculations is rigorous and does not involve weighting functions, nor does it impose additional constraints on the problem unlike the weighted function or the epsilon correction method.

Let $\sum_{t_i=0}^{t_i=t_f} q_j(t_i)$ ($j=1..n$) be the variables that need to be minimized/maximized simultaneously for a problem involving a set of ODE

$$\frac{dx}{dt} = F(x, u) \quad (11)$$

t_f being the final time value and n the total number of objective variables. u is the control parameter. The MNL MPC method first solves the single objective optimal control problem

independently optimizing each of the variables $\sum_{t_i=0}^{t_i=t_f} q_j(t_i)$

individually. The minimization/maximization of $\sum_{t_i=0}^{t_i=t_f} q_j(t_i)$ will lead to the values q_j^* . Then the optimization problem that will be solved is

$$\min \left(\sum_{j=1}^n \left(\sum_{t_i=0}^{t_i=t_f} q_j(t_i) - q_j^* \right)^2 \right) \\ \text{subject to } \frac{dx}{dt} = F(x, u); \quad (12)$$

This will provide the values of u at various times. The first obtained control value of u is implemented and the rest are discarded. This procedure is repeated until the implemented and the first obtained control values are the same or if the Utopia point or if the Utopia point ($\sum_{t_i=0}^{t_i=t_f} q_j(t_i) = q_j^*$) for all j . is obtained.

The optimization package in Python, Pyomo⁵⁸, where the differential equations are automatically converted to a Nonlinear Program (NLP) using the orthogonal collocation method will be used. The resulting nonlinear optimization problem was solved using the solvers IPOPT⁵⁹ and confirmed as a global solution with BARON⁶⁰. To summarize the steps of the algorithm are as follows

Optimize $\sum_{t_i=0}^{t_i=t_f} q_j(t_i)$ subject to the differential and algebraic equations that govern the process using Pyomo with IPOPT and

BARON. This will lead to the value q_j^* at various time intervals t_i . The subscript i is the index for each time step.

Minimize $\left(\sum_{j=1}^n \left(\sum_{t_i=0}^{t_i=t_f} q_j(t_i) - q_j^* \right)^2 \right)$ subject to the differential and algebraic equations that govern the process using Pyomo with IPOPT and BARON. This will provide the control values for various times.

Implement the first obtained control values and discard the remaining.

Repeat steps 1 to 3 until there is an insignificant difference between the implemented and the first obtained value of the control variables or if the Utopia point is achieved. The Utopia

point is when $\sum_{t_i=0}^{t_i=t_f} q_j(t_i) = q_j^*$ for all j .

Sridhar⁶¹ proved that the MNL MPC calculations to converge to the Utopia solution when the bifurcation analysis revealed the presence of limit and branch points. The Utopia point is when $\sum_{t_i=0}^{t_i=t_f} p_j(t_i) = p_j^*$ for all j . This was done by imposing the singularity condition on the co-state equation (Upreti, 2013). If the minimization be of the variable q_1 lead to the value

q_1^* and the minimization of function q_2 lead to the value q_2^* . The MNLPMC calculations will minimize the function $(q_1 - q_1^*)^2 + (q_2 - q_2^*)^2$. The Mult objective optimal control problem is

$$\min (q_1 - q_1^*)^2 + (q_2 - q_2^*)^2 \quad \text{subject to} \quad \frac{dx}{dt} = F(x, u) \quad (13)$$

$$\frac{d}{dx_i} ((q_1 - q_1^*)^2 + (q_2 - q_2^*)^2) = 2(q_1 - q_1^*) \frac{d}{dx_i} (q_1 - q_1^*) + 2(q_2 - q_2^*) \frac{d}{dx_i} (q_2 - q_2^*) \quad (14)$$

The Utopia point requires that both $(q_1 - q_1^*)$ and $(q_2 - q_2^*)$ are zero. Hence

$$\frac{d}{dx_i} ((q_1 - q_1^*)^2 + (q_2 - q_2^*)^2) = 0 \quad (15)$$

the optimal control co-state equation⁶² is

$$\frac{d}{dt} (\lambda_i) = -\frac{d}{dx_i} ((q_1 - q_1^*)^2 + (q_2 - q_2^*)^2) - f_x \lambda_i; \quad \lambda_i(t_f) = 0 \quad (16)$$

λ_i is the Lagrangian multiplier. t_f is the final time. The first term in this equation is 0 and hence

$$\frac{d}{dt} (\lambda_i) = -f_x \lambda_i; \quad \lambda_i(t_f) = 0 \quad (17)$$

At a limit or a branch point, for the set of ODE $\frac{dx}{dt} = f(x, u)$ f_x is singular. Hence there are two different vectors-values for $[\lambda_i]$ where $\frac{d}{dt} (\lambda_i) > 0$ and $\frac{d}{dt} (\lambda_i) < 0$. In between there is a vector $[\lambda_i]$ where $\frac{d}{dt} (\lambda_i) = 0$. This coupled with the boundary condition $\lambda_i(t_f) = 0$ will lead to $[\lambda_i] = 0$. This makes the problem an unconstrained optimization problem and the only solution for the unconstrained problem is the Utopia solution.

Results and Discussion

For problem 1, pa was used as the bifurcation parameter and a branch point (BP), limit point (LP) and a Hopf bifurcation point (HP) were found at (ax, ay, az, pa) values of (0.000000 0.000000 1.000000 0.355000); (0.021015 0.027565 0.612369 0.324949) and (0.019563 0.060804 0.171749 0.551033); values respectively. This is shown in (Figure 1 and Figure 2) shows the limit cycle arising from the Hopf bifurcation point. Sridhar⁶³ showed that the Hopf bifurcation point would be eliminated by the use of an activation factor involving the tanh function. This was because the tanh function increases the time period of the oscillatory behavior which occurs in the form of a limit cycle caused by Hopf bifurcations.

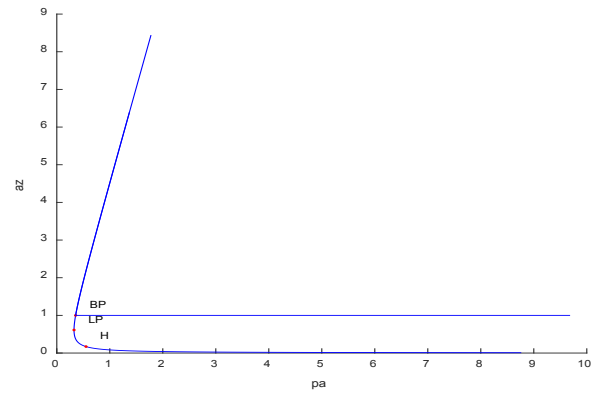


Figure 1: Branch point, limit points and Hopf bifurcation points for problem 1

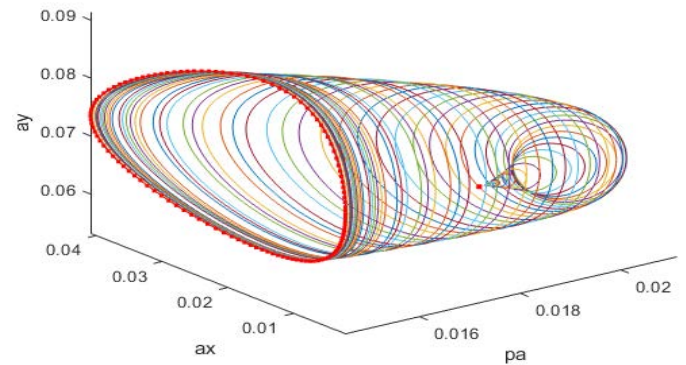


Figure 2: Limit cycle arising from the Hopf bifurcation point in Problem 1

When pa was modified to $\text{pa} \cdot (\tanh(\text{pa}))/0.02$ the Hopf bifurcation point disappeared (Figure 3) confirming the correctness of the analysis of Sridhar⁶³. In problem 2, q was the bifurcation parameter and a branch point was located at [xa, ya, za, wa, q] values (0.0 1.222222 0.0 100.000000 1.344444). (Figure 4) In problem 3 η_p is the bifurcation parameter and a branch point was located at (tval, cval, pval, bval, η_p) values of (0.000000 0.000000 0.714286 0.000000 0.014000) (Figure 5).

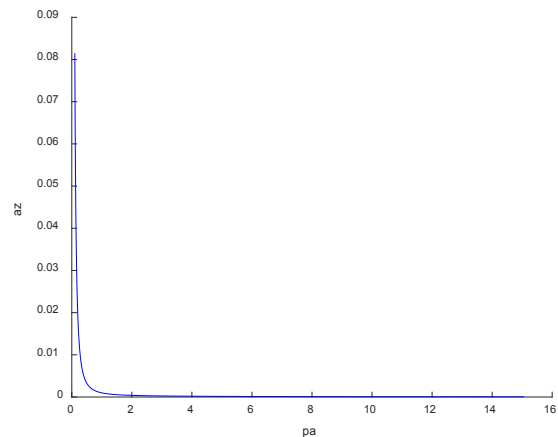


Figure 3: Hopf bifurcation point disappears when pa was modified to $\text{pa} \cdot \tanh(\text{pa})/0.02$

Limit/Branch points were found in all three problems. Sridhar⁶¹ showed that the presence of the limit and branch points enabled the MNLPMC calculations to converge to the Utopia solution. This result is confirmed in the MNLPMC calculations for all the three problems,

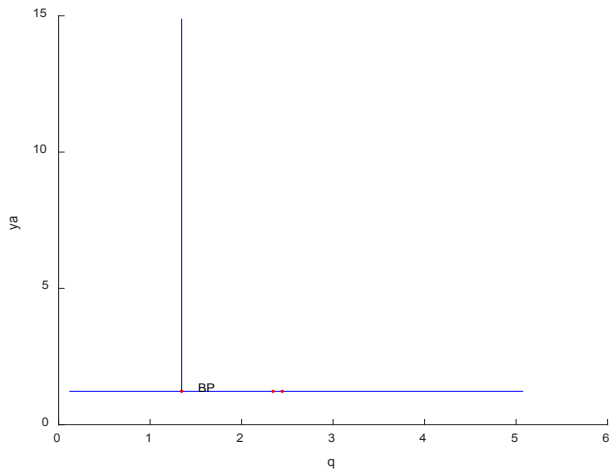


Figure 4: Bifurcation diagram for problem 2.

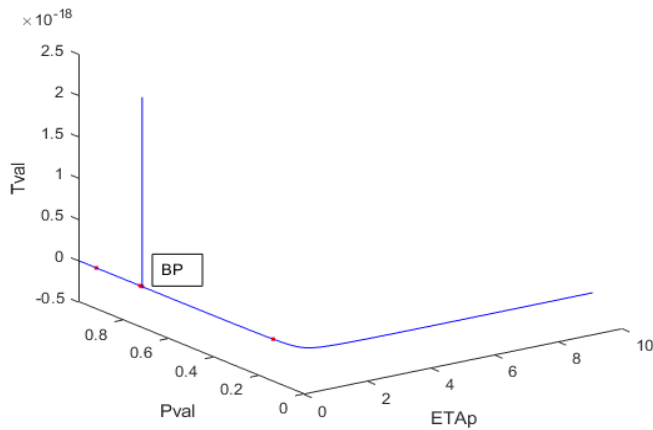


Figure 5: Bifurcation Diagram for problem 3.

In problem 1, $\sum_{t=0}^{t=tf} ax + \sum_{t=0}^{t=tf} ay$ was maximized and this maximization resulted in a value of $11.0697 \sum_{t=0}^{t=tf} az$ was minimized and this minimization resulted in a value of 0. The overall minimization involved the objective function $(\sum_{t=0}^{t=tf} ax + \sum_{t=0}^{t=tf} ay - 11.0697 \sum_{t=0}^{t=tf} az)^2 + (\sum_{t=0}^{t=tf} az)^2$. This minimization resulted in the Utopia point 0. The first obtained control value was implemented and the remaining discarded. This procedure was repeated until the difference between the first and second control values was negligible, the obtained control value (MNLMPc value) of pa was 2.45771905. The MNLMPc profiles of ax, ay, az and pa are shown in (Figure 6).

In problem 2, $\sum_{t=0}^{t=tf} za$ was maximized and this maximization resulted in a value of $24.78026859 \sum_{t=0}^{t=tf} ya$ was minimized and this minimization resulted in a value of 0. The overall minimization involved the objective function $(\sum_{t=0}^{t=tf} za - 24.78026859 \sum_{t=0}^{t=tf} ya)^2 + (\sum_{t=0}^{t=tf} ya)^2$. This minimization resulted in the Utopia point 0. The control variable was q/ The first obtained control value was implemented and the remaining discarded. This procedure was repeated until the difference

between the first and second control values was negligible, the obtained control value (MNLMPc value) of q was 4.99999. (Figures 7-10) show the various MNLMPc profiles.

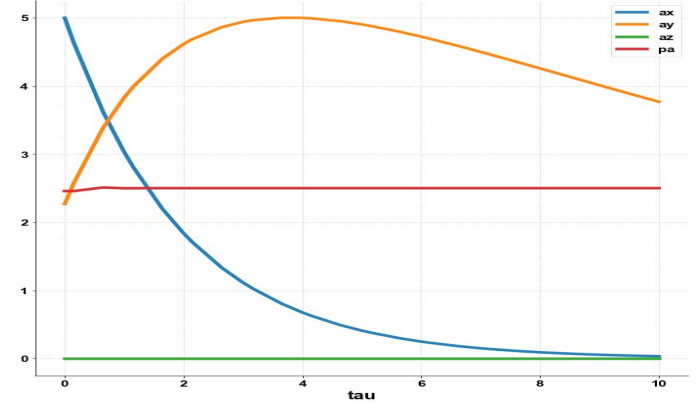


Figure 6: MNLMPc profiles of ax, ay, az and pain Problem 1.

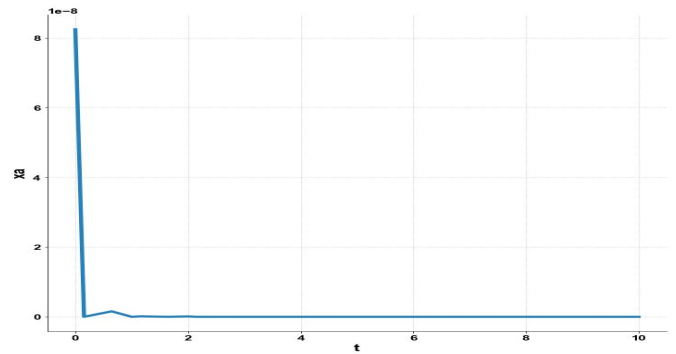


Figure 7: MNLMPc profile of xa in problem 2.

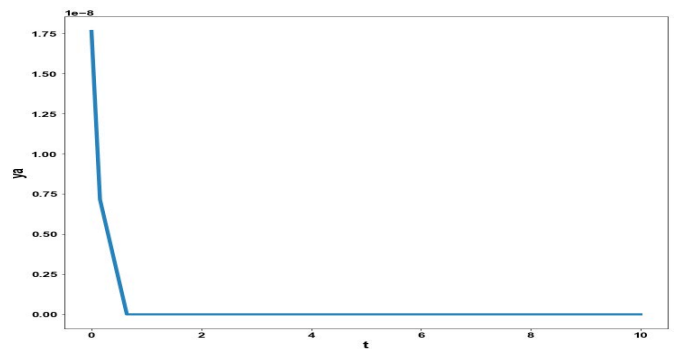


Figure 8: MNLMPc profile of ya in problem 2.

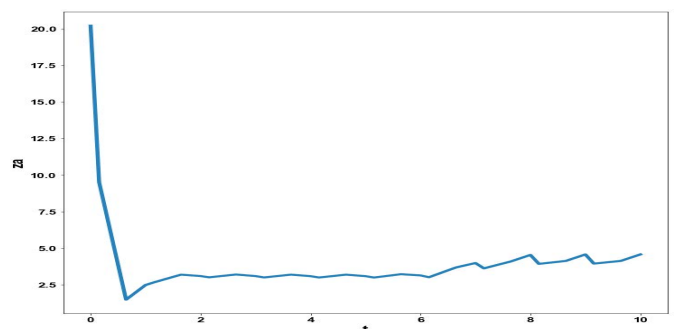


Figure 9: MNLMPc profile of za in problem 2

The obtained control profile of q exhibited a lot of noise (Figure11). This was remedied using the Savitzky-Golay Filter. The Savitzky-Golay filter, is a digital filter widely used for data smoothing and differentiation. The Savitzky-Golay filter maintains the integrity of the original signal preserving the shape and features of the signal. The smoothed-out version of this profile is shown in (Figure 12).

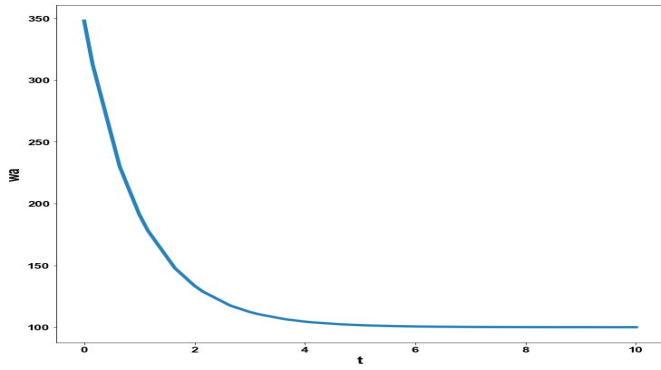


Figure 10: MNLMP profile of wa in problem 2.

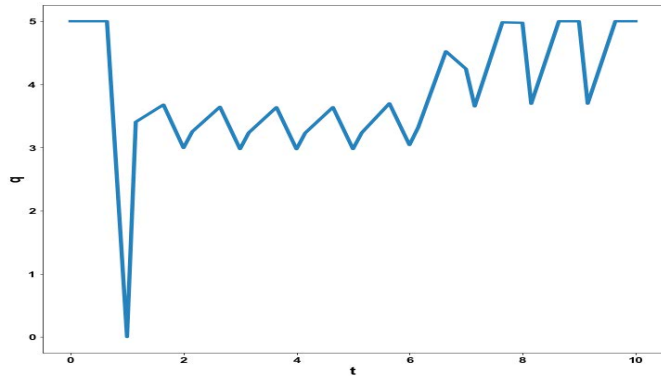


Figure 11: MNLMP profile of q in problem 2.

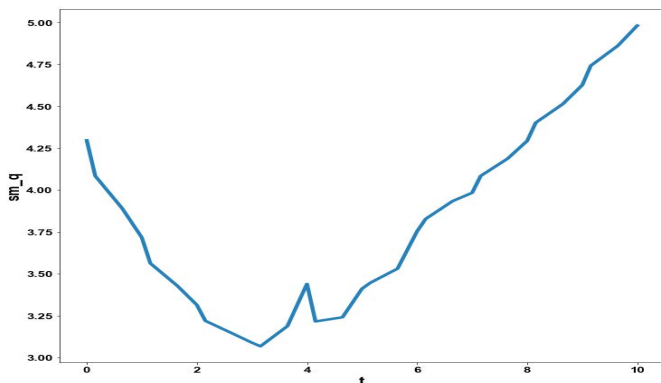


Figure 12: MNLMP profile of q in problem 2 with noise removed with Savitsky Golay Filter.

In problem 3, η_p was the control variable, $\sum_{t=0}^{t=10} cval$ was maximized and this maximization resulted in a value of 1000. $\sum_{t=0}^{t=10} tval$ was inimized and this minimization resulted in a value of 0. The overall minimization involved the objective function $(\sum_{t=0}^{t=10} cval - 1000)^2 + (\sum_{t=0}^{t=10} tval)^2$. This minimization resulted in the Utopia point 0. The first obtained control value was implemented and the remaining discarded. This procedure was repeated until the difference between the first and second control values was negligible, The obtained control value (MNLMP value) of η_p was 3.7797402436111.

(Figures 13-16) show the various MNLMP profiles. The obtained control profile of q exhibited a lot of noise (Figure 17). This was remedied using the Savitzky-Golay Filter. The smoothed-out version of this profile is shown in (Figure 18). The

results in the three problems confirm the analysis of Sridhar⁶¹ who showed that the presence of the limit and branch points enabled the MNLMP calculations to converge to the Utopia solution. Problem 1 exhibits a Hopf bifurcation point. Sridhar⁶³ showed that the Hopf bifurcation point would be eliminated by the use of an activation factor involving the tanh function. In problem 1, when pa was modified to $pa \cdot (\tanh(pa))/0.02$ the Hopf bifurcation point disappeared confirming the analysis of Sridhar⁶³.

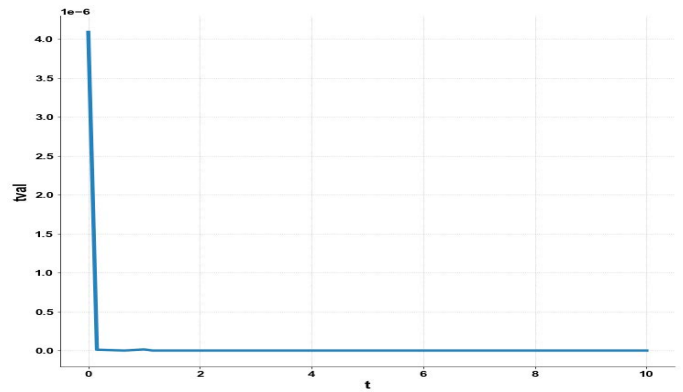


Figure 13: MNLMP profile of tval in problem 3.

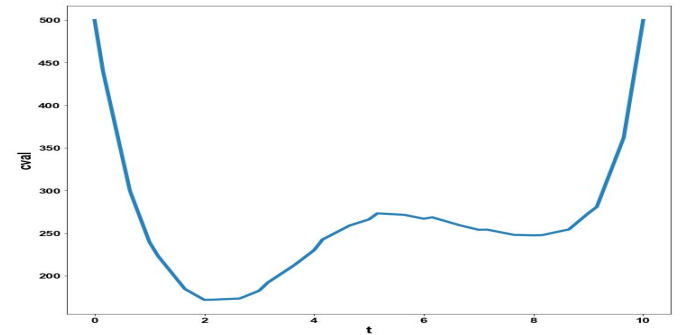


Figure 14: MNLMP profile of cval in problem 3.

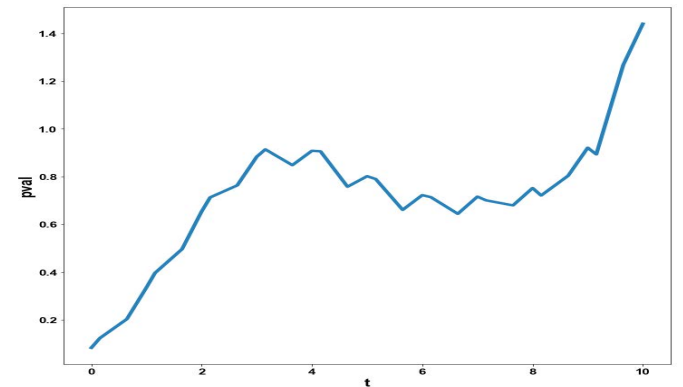


Figure 15: MNLMP profile of pval in problem 3.

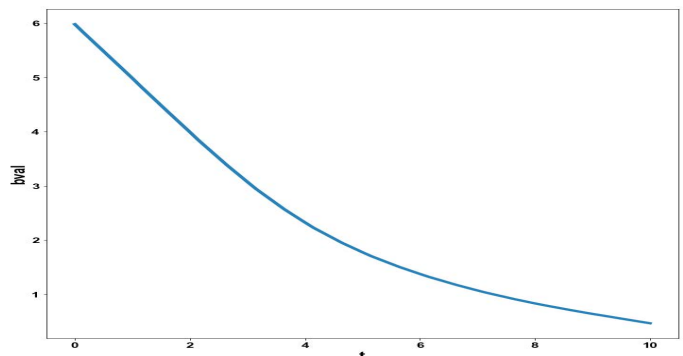


Figure 16: MNLMP profile of bval in problem 3

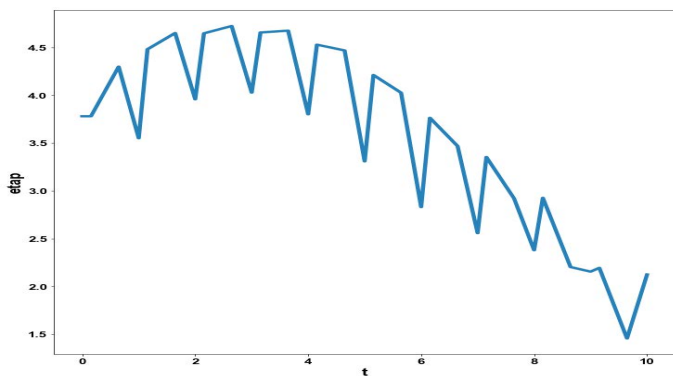


Figure 17: MNL MPC profile of in problem 3.

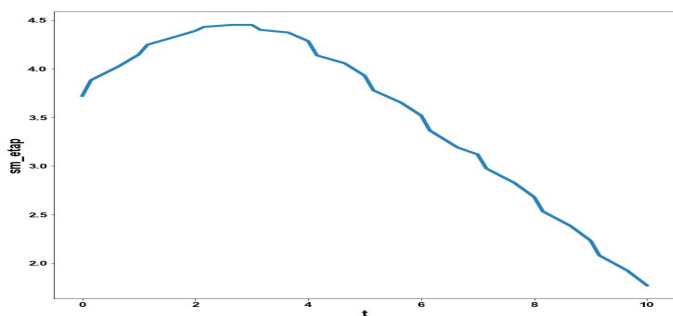


Figure 18: MNL MPC profile of in problem 3 with noise removed with Savitsky Golay Filter.

Conclusion

Rigorous bifurcation analysis and Mult objective nonlinear model predictive control calculations were performed on models involving CAR-T cells. The bifurcation analysis revealed limit points branch points and Hopf bifurcation points. The Hopf bifurcation points that cause unwanted limit cycles were eliminated using an activation factor involving the tanh function. The limit and branch points were beneficial because they allowed the Mult objective nonlinear model predictive control calculations to converge to the Utopia point which is the best solution.

Data Availability Statement

All data used is presented in the paper.

Conflict of Interest

The author, Dr. Lakshmi N Sridhar has no conflict of interest.

References

- De Boer RJ, Oprea M, Antia R, Murali-Krishna K, Ahmed R and Perelson AS. Recruitment times, proliferation and apoptosis rates during the cd8+ t-cell response to lymphocytic choriomeningitis virus. *J Virology* 2001;75(22):10663-10669.
- Antia R, Bergstrom CT, Pilyugin SS, Kaech SM and Ahmed R. Models of cd8+ responses: 1. what is the antigen-independent proliferation program. *J Theoretical Bio* 2003;221(4):585-598.
- Antia R, Ganusov VV and Ahmed R. The role of models in understanding cd8+ t-cell memory. *Nature Reviews Immunology* 2005;5(2):101-111.
- de Pillis LG, Radunskaya AE and Wiseman CL. A validated mathematical model of cell-mediated immune response to tumor growth. *Cancer research* 2005;65(17):7950-7958.
- Brentjens R, Yeh R, Bernal Y, Riviere I, Sadelain M. Treatment of chronic lymphocytic leukemia with genetically targeted autologous T cells: Case report of an unforeseen adverse event in a phase I clinical trial. *Mol Ther* 2010;18:666-668.
- Kalos M, Levine BL, Porter DL, Katz S, Grupp SA, Bagg A, June CH. Cells with chimeric antigen receptors have potent antitumor effects and can establish memory in patients with advanced leukemia. *Sci Transl Med* 2011;3.
- Kochenderfer JN, Dudley ME, Feldman SA, et al. B-cell depletion and remissions of malignancy along with cytokine-associated toxicity in a clinical trial of anti-CD19 chimeric-antigen-receptor transduced T cells. *Blood* 2012;119:2709-2720.
- Grupp SA, Kalos M, Barrett D, Aplenc R, Porter DL, Rheingold SR, Teachey DT, Chew A, Hauck B, Wright JF. Chimeric antigen receptor-modified t cells for acute lymphoid leukemia. *New Eng J Med* 2013;368(16):1509-1518.
- De Boer RJ and Perelson AS. Quantifying t lymphocyte turnover. *J theoretical biology* 2013;327:45-87.
- Dotti G, Gottschalk S, Savoldo B, Brenner MK. Design and development of therapies using chimeric antigen receptor-expressing T cells. *Immunol Rev* 2014;257:107-126.
- Davenport AJ, Jenkins MR, Ritchie S, Prince HM, Trapani JA, Kershaw MH, Darcy PK, Neeson PJ. CAR-T cells are serial killers. *Oncoimmunology* 2015;4:1053684.
- Brown CE, Alizadeh D, Starr R, et al. Regression of glioblastoma after chimeric antigen receptor t-cell therapy. *N Engl J Med* 2016;375(26):2561-2569.
- Brown C, Aguilar B, Starr R, et al. Optimization of il13ra2-targeted chimeric antigen receptor t cells for improved persistence and antitumor efficacy against glioblastoma *Mol Therapy* 2017.
- Hege KM, Bergsland EK, Fisher GA, Nemunaitis JJ, Warren RS, McArthur JG, Lin AA, Schlom J, June CH, Sherwin SA. Safety, tumor trafficking and immunogenicity of chimeric antigen receptor (car)-t cells specific for tag-72 in colorectal cancer. *J Immunother Cancer* 2017.
- Davenport AJ, Cross RS, Watson KA, et al. Chimeric antigen receptor T cells form nonclassical and potent immune synapses driving rapid cytotoxicity. *Proc Natl Acad Sci USA* 2018;115:2068-2076.
- Mostolizadeh R, Afsharnezhad Z, Marciniak-Czochra A. Mathematical model of chimeric antigen receptor (CAR) T cell therapy with presence of cytokine. *Numer Algebr Control Optim* 2018;8:63-80.
- Stein AM, Grupp SA, Levine JE, et al. Tisagenlecleucel model-based cellular kinetic analysis of chimeric antigen receptor-t cells. *CPT: pharmacometrics systems pharma* 2019;8(5):285-295.
- Shah NN and Fry TJ. Mechanisms of resistance to CAR T cell therapy. *Nat Rev Clin Oncol* 2019;16(6):372-385.
- Feins S, Kong W, Williams EF, Milone MC, Fraietta JA. An introduction to chimeric antigen receptor (car) t-cell immunotherapy for human cancer. *Am J Hematol* 2019;94(1):3-9.
- Ghorashian S, Kramer A, Onuoha S, et al. Enhanced car t cell expansion and prolonged persistence in pediatric patients with all treated with a low-affinity cd19 car. *Nat Med* 2019;25(5):1408-1414.
- Chavez JC, Bachmeier C, Khafan-Dabaja MA. Car t-cell therapy for b-cell lymphomas: clinical trial results of available products. *Therap Adv Hematol* 2019;10:2040620719841581.
- Bodnar M, Piotrowska MJ, Bogdańska MU. Mathematical analysis of a generalized model of chemotherapy for low grade gliomas. *Discrete Contin Dyn Syst B* 2019;24(5):2149-2167.
- Barros LRC, Rodrigues BJ, Almeida RC. CAR-T cell goes on a mathematical model. *J Cell Immunol* 2020;2(1)31-37.
- Chaudhury A, Zhu X, Chu L, Goliaei A, June CH, Kearns JD and Stein AM. Chimeric antigen receptor t cell therapies: a review

- of cellular kinetic-pharmacodynamic modeling approaches. The Journal of Clinical Pharmacology 2020;60:147-159.
25. Vercellino L, Blasi RD, Kanoun S, et al. Predictive factors of early progression after car t-cell therapy in relapsed/refractory diffuse large b-cell lymphoma. Blood advances 2020;4(22):5607-5615.
 26. Altrock PM, Kimmel GJ, Locke FL. The roles of t cell competition and stochastic extinction events in chimeric antigen receptor t cell therapy. Proceedings. Biological sciences 2021;288:1947.
 27. Liu C, Ayyar VS, Zheng X, et al. Model-based cellular kinetic analysis of chimeric antigen receptor-t cells in humans. Clin Pharmacol Therapeutics 2021;109(3):716-727.
 28. Martínez-Rubio A, Chulián S, Blázquez Goñi MROC, et al. A mathematical description of the bone marrow dynamics during car t-cell therapy in b-cell childhood acute lymphoblastic leukemia. Int J Mol Sci 2021;22:6371.
 29. Barros LRC, Paixão EA, Valli AMP, Naozuka GT, Fassoni AC, Almeida RC. CART math-a mathematical model of CAR-T immunotherapy in preclinical studies of hematological cancers. Cancers 2021;13(12):2941.
 30. Mueller-Schoell A, Puebla-Osorio N, Michelet R, et al. Early survival prediction framework in cd19-specific car-t cell immunotherapy using a quantitative systems pharmacology model. Cancers 2021;13(11):2782.
 31. Singh AP, Chen W, Zheng X, Mody H, Carpenter TJ, Zong A, Heald DL. Bench-to bedside translation of chimeric antigen receptor (car) t cells using a multiscale systems pharmacokinetic-pharmacodynamic model: a case study with anti-bcma car-t. CPT: Pharmacometrics & Systems Pharmacology 2021;10(4):362-376.
 32. Pérez-García VM, León-Triana O, Rosa M, Perez-Martinez A. Car t cells for t-cell leukemias: Insights from mathematical models. Communications in Nonlinear Science and Numerical Simulation 2021;96:105684.
 33. Kimmel GJ, Locke FL, Altrock PM. The roles of T cell competition and stochastic extinction events in chimeric antigen receptor T cell therapy. Proc Roy Soc B Biol Sci 2021;288(1947):20210229.
 34. León-Triana O, Perez-Martinez A, Ramirez-Orellana M, Perez-García V. Dual-target car-ts with on- and off-tumor activity may override immune suppression in solid cancers: a mathematical proof of concept. Cancers 2021;13(4):703.
 35. León-Triana O, Soukaina S, Calvo G, Belmonte-Beitia J, Chulián S, Martínez-Rubio A, Rosa M, Pérez-Martínez A, Ramirez-Orellana M, Pérez-García V. Car t cell therapy in b-cell acute lymphoblastic leukemia: insights from mathematical models. Commun. Nonlinear Sci Numer Simul 2021;94:105570.
 36. Liu C, Ayyar VS, Zheng X, Chen W, Zheng S, Mody H, Wang W, Heald D, Singh AP, Cao Y. Model-based cellular kinetic analysis of chimeric antigen receptor-T cells in humans. Clin Pharmacol Therap 2021;109(3):716-727.
 37. Martínez-Rubio Á, Chulián S, Blázquez Goñi C, et al. A mathematical description of the bone marrow dynamics during car t-cell therapy in b-cell childhood acute lymphoblastic leukemia. Int J Mol Sci 2021;22(12):6371.
 38. Nukala U, Rodriguez Messan M, Yogurtcu ON, Wang X, Yang H. A systematic review of the efforts and hindrances of modeling and simulation of CAR T-cell therapy. AAPS J 2021;23(3):52.
 39. Owens K, Bozic I. Modeling CAR T-cell therapy with patient preconditioning. Bull Math Biol 2021;83(5):42.
 40. Valle PA, Coria LN, Plata C, Salazar Y. CAR-T cell therapy for the treatment of ALL: eradication conditions and in silico experimentation. Hemato 2021;2(3):441-462.
 41. Santurio DS, Barros LRC. A mathematical model for on-target off-tumor effect of car-t cells on gliomas. Front Syst Biol 2022.
 42. Paixão EA, Barros LRC, Fassoni AC, Almeida RC. Modeling patient-specific car-t cell dynamics: Multiphasic kinetics via phenotypic differentiation. Cancers 2022;14(22):5576.
 43. Salem AM, Mugundu GM, Singh AP. Development of a multiscale mechanistic modeling framework integrating differential cellular kinetics of car t-cell subsets and immunophenotypes in cancer patients. CPT: Pharmacometrics Sys Pharmacol 2023;12(9):1285-1304.
 44. Kirouac DC, Zmurchok C, Deyati A, Sicherman J, Bond C, Zandstra PW. Deconvolution of clinical variance in car-t cell pharmacology and response. Nat biotechno 2023:1-12.
 45. Bodnar M, Forys U, Piotrowska MJ, Bodzioch M, Romero-Rosales JA, Belmonte-Beitia J. On the analysis of a mathematical model of car-t cell therapy for glioblastoma: insights from a mathematical model. Int J Appl Math Comput Sci 2023;33(3):379-394.
 46. Santurio DS, Paixão EA, Barros LRC, Almeida RC, Fassoni AC. Mechanisms of resistance to car-t cell immunotherapy: Insights from a mathematical model. Appl Mathematical Model 2024;125:1-15.
 47. Serrano S, Barrio R, Martínez-Rubio A, Belmonte-Beitia J, Pérez-García VM. Understanding the role of b-cells in car t-cell therapy in leukemia through a mathematical mode 2024.
 48. Santurio DS, Barros LRC, Glauche I, Fassoni AC. Mathematical modeling unveils the timeline of car-t cell therapy and macrophage-mediated cytokine release syndrome. BioRxiv 2024;2024.
 49. Fassoni AC, Braga DC. Nonlinear dynamics of CAR-T cell therapy 2024.
 50. Khailov E, Grigorieva E, Klimenkova A. Optimal CAR T-cell Immunotherapy Strategies for a Leukemia Treatment Model. Games 2020;11(4):53.
 51. Marek B, Joanna MP, Mariusz B, Belmonte-Beitia J, Urszula F. Dual CAR-T cell therapy for glioblastoma: strategies to cure tumor diseases based on a mathematical model Nonlinear Dynamics 2025;113:1637-1666.
 52. Dhooge A, Govaerts W and Kuznetsov AY. MATCONT: A Matlab package for numerical bifurcation analysis of ODEs, ACM transactions on Mathematical software 2003;29(2):141-164.
 53. Dhooge A, Govaerts W, Kuznetsov YA, Mestrom W, Riet AM. CL_MATCONT; A continuation toolbox in Matlab 2004.
 54. Kuznetsov YA. Elements of applied bifurcation theory. Springer, NY 1998.
 55. Kuznetsov YA. Five lectures on numerical bifurcation analysis, Utrecht University, NL 2009.
 56. Govaerts WJF. Numerical Methods for Bifurcations of Dynamical Equilibria, SIAM 2000.
 57. Flores-Tlacuahuac A. Pilar Morales, Martin Rivalto Toledo; Mult objective Nonlinear model predictive control of a class of chemical reactors. IEC research 2012:5891-5899.
 58. William EH, Laird CD, Watson J. Pyomo - Optimization Modeling in Python. Second Edition 2017;67.
 59. Wächter A, Biegler L. On the implementation of an interior-point filter line-search algorithm for large-scale nonlinear programming. Math. Program 2006;106:25-57.
 60. Tawarmalani M, Sahinidis NV. A polyhedral branch-and-cut approach to global optimization, Mathematical Programming 2005;103(2):225-249.
 61. Sridhar LN. Coupling Bifurcation Analysis and Mult objective Nonlinear Model Predictive Control. Austin Chem Eng 2024;10(3):1107.

62. Ranjan US. Optimal control for chemical engineers. Taylor and Francis 2013
63. Sridhar LN. Elimination of oscillation causing Hopf bifurcations in engineering problems. J Appl Math 2024;2(4):1826.